UDC 620.178.16:621.921.34-488:621.793.3

Kong Dejun*, Zhao Wen, Zhang Ling
School of Mechanical Engineering, Changzhou University,
Changzhou, China
**kong-dejun@163.com*

Friction-wear behaviors of chemical vapor deposited diamond films at high temperatures

A diamond film was deposited on YT14 hard alloy cutting tool using a chemical vapor deposition. The coefficients of friction and wear behaviors of the obtained diamond films at 500, 600, and 700 ℃ were investigated using a high temperature tribological tester. The results show that the C of diamond film is fully released at 700 ℃, generating CO and CO_2. The (220) plane of diamond film is oxidized fully at 500 ℃, while the (110) plane of diamond film is oxidized at 700 ℃. The average coefficients of friction of diamond film at 500, 600 and 700 ℃ are 0.55, 0.49, and 0.48, respectively, the wear mechanism is primarily oxidation wear, adhesive wear and abrasive wear, accompanied with fatigue wear.

Keywords*: chemical vapor deposition (CVD), diamond film, coefficient of friction, high temperature, friction and wear, wear mechanism.*

INTRODUCTION

Diamond film has many advantages such as high hardness [1], wear resistance [2], high thermal stability [3], and etc., which is extensively used on cutting tools [4, 5]. In this case, understanding the wear characteristics of coatings at high temperatures is essential for advanced manufacturing engineering [6–9]. The diamond film is inert at normal temperature, while it is oxidized at high temperature, which leads to failing and destroys the protected cutting tools [10–11] due to its chemical reactions [12]. The working temperature of chemical vapor deposited diamond film is nearly equaled to that of the natural diamonds, which is oxidized at 800–900 °C. The oxidation temperature and rates of chemical vapor deposited diamond film are associated with the defects on its surface, such as dislocation, impurities, twins etc., which cause oxidation resistance of chemical vapor deposited diamond film lower than that of natural diamond [13–15]. The friction-wear performances of diamond film have been extensively studied, Qian et al. [16] reported that the diamond film with the binder of magnesium carbonate behaved a higher wear resistance than that of diamond film with cobalt binder; Konicek et al. [17] investigated the frictional properties of ultrananocrystalline diamond film; Sun et al. [18] discovered that the nano-diamond was far superior than the single-pose nano-diamond; Shabani et al. [19] found the average COF of diamond film was 0.64. However, the friction-wear behaviors of chemical vapor deposited diamond film at high temperatures have rarely reported. In this study, a diamond film was deposited on YT14 hard alloy with using a chemical vapor deposition (CVD), the COF of obtained film was investigated using a high temperature tribological tester. The surface morphologies, chemical elements, and phases of worn tracks were analyzed using a scanning electron microscope (SEM), energy dispersive

spectroscope (EDS), and X-ray diffraction (XRD), respectively, which provided an experimental basis for the chemical vapor deposited diamond film applying on the surface modification of cutting tools.

EXPERIMENTAL

The substrate was marketed YT14 hard alloy cutting tool with the following chemical composition (wt %): WC 78, TiC 14, Co 8. The samples were polished by 80#, 120#, 200# and 600# sandpapers and metallographic sandpaper, respectively. The samples were cleaned with pure acetone in an ultrasonic oscillation for 10 min and were dried before being putted into the configured chemical vapor deposited chamber. The deposition procedure was shown as followed: (1) carbon source gas → CH_4 (corresponding to 0.5–10 vol %) → and H_2 was bubbled into a vacuum deposition chamber (2). The huge of $–CH_3$ interacted with each other at the high temperature of 800 °C and low pressure of 4.3×10^{-3} Pa, then C was linked with each other via covalent bonds. (3) With the deposition continuing, the diamond nucleation was formed on the substrate surface and the H in the nucleation was replaced by $–CH_3$. (4) The deposition of diamond film was finished. The friction-wear test of diamond film was conducted on a HT–1000 type high temperature tribological tester, the wear parameters: friction mode of sliding, tribo–pair ceramic balls (Si_3N_4) with the diameter of 6 mm, load of 3 N, rotating speed of 500 rpm, rotation radius of 5 mm, respective test temperatures: 500, 600, and 700 °C. After the wear tests, the samples were cleaned in alcohol to remove the dust, and rinsed with deionized water for 15 min and dried using a heater. The morphologies, chemical elements, and phases of worn tracks were analyzed using a JSM-6360LA type SEM, its configured EDS and D/max type XRD, respectively.

ANALYSIS AND DISCUSSION OF RESULTS

Morphologies, AFM, EDS analysis and mechanical properties of diamond films

Figure 1, *a* shows the morphologies of diamond film surface. The film was continuously dense, and there were no uncoated pits, which was credited to be great protected film. Figure 1, *b* shows the morphologies of film interface. The film was smooth, no distinguished peaks, showing that the diamond was deposited on the substrate, and there was a divided layer between the film and the substrate, of which the upper layer was the diamond film with the thickness ~600 nm, and the low layer was the substrate. The AFM topography of diamond film with the size of 10000×10000 nm is shown in Fig. 1, *c*. The surface roughness S_a of diamond film was 79.2 nm, which meant the film was smooth. The EDS analysis result of diamond film is shown in Fig. 1, *d*, the mass fractions (wt %): C – 52.49, Ti – 12.67 and W – 34.85; and the corresponding atom fractions (at %): C – 86.84, Ti – 5.26, and W – 7.90. The film was primarily composed of C, while the W and Ti came from chemical elements of substrate, measured by X-ray penetrating the film.

XRD analysis

Figure 2 shows the XRD patterns of diamond film at normal temperature, 500, 600, and 700 °C. In Fig. 2, *a*, the peaks at $2\theta = 44.1°$, 75.4° represented the diffraction plane (111) and (220) of diamond film, respectively [20]. This meant the diamond film had complete crystal structure and its lattice parameters were consistent with natural diamond. The (111) plane was more intense than the (220) plane, which revealed that the crystal shape was the (111) plane. Therefore, the diamond film began to oxidize partially, the (220) plane primarily was oxidized at

500 °C. The peaks in Fig. 2, *c* were similar with those in Fig. 2, *b*, revealing that the rest (111) plane was not oxidized at 600 °C. There was only the WO_3 in the XRD patterns of diamond film at 700 °C in Fig. 2, *d*, showing that the diamond film was oxidized fully, the WC in the substrate was oxidized as well and produced WO_3. The W had a strong affinity to the O, and the Gibbs free energy required for forming the WO_3 was lower than that of TiO_2, therefore, the oxides were primarily WO_3 [21]. The reactions were shown as follows:

$$2WC + 5O_2 = 2WO_3 + 2CO_2\uparrow; \quad (1)$$

$$WC + 2O_2 = WO_3 + CO\uparrow. \quad (2)$$

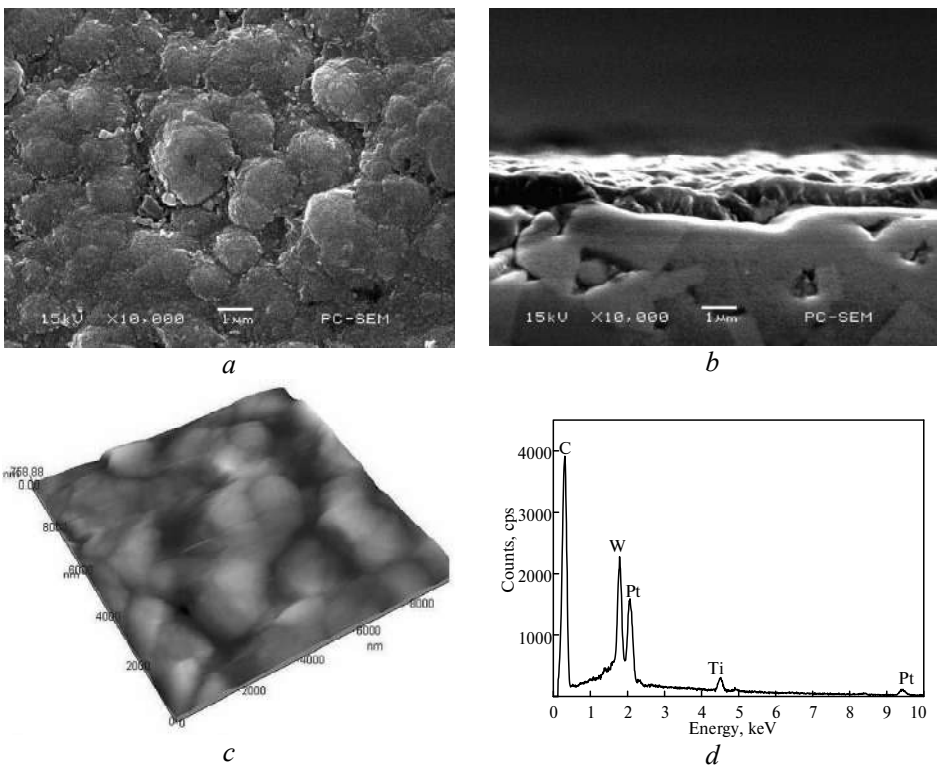

Fig. 1. Surface (*a*) and interface (*b*) morphologies, AFM (*c*) and EDS (*d*) analysis of diamond film.

Analysis of COFs

Figure 3 shows the relationship between the COFs of diamond films and wear time at 500, 600, 700 °C. At 500 °C, the average COF in the running-in period and stable period was 0.54 and 0.56, respectively, which was nearly close to the average COF of 0.55 in the overall wear period. This was because the film was not completely oxidized, which made it difficult to be worn out. At 600 °C, the average COF of diamond film was 0.49, decreased by 10.91 %, when compared with that at 500 °C. The average COF at the running-in period was 0.54, which was the same as that at 500 °C, whereas the COF at stable period was 0.47, decreased by 12.96 %. The gathered debris on the worn track increased the shearing stress, which caused the COFs to fluctuate at the stable period. At 700 °C, the diamond film was completely oxidized and produced a large amount of CO_2 and CO at 700 °C, the average COF of diamond film was 0.48, while that in the running-in

period was 0.50, decreased by 7.40 % compared with that at 500 °C. With the wear continuing, the CO_2 and CO oxides increased, decreasing friction resistance; the fluctuation of COFs at 600 and 700 °C tended to across each other. With the increase of wear temperature, the average COFs of diamond film decreased, because the film didn't reach the oxidation temperature at 500 °C and was still intact. At 600 °C, the diamond film started to oxide partly on the worn track. After the surface particles disappearing, the actual contacted area increased, the COF began to decline slowly and tended to be stable. At 700 °C, the diamond film was oxidized fully in few minute, the tribopair of Si_3N_4 ball directly contacted with substrate, the COF curve became smooth.

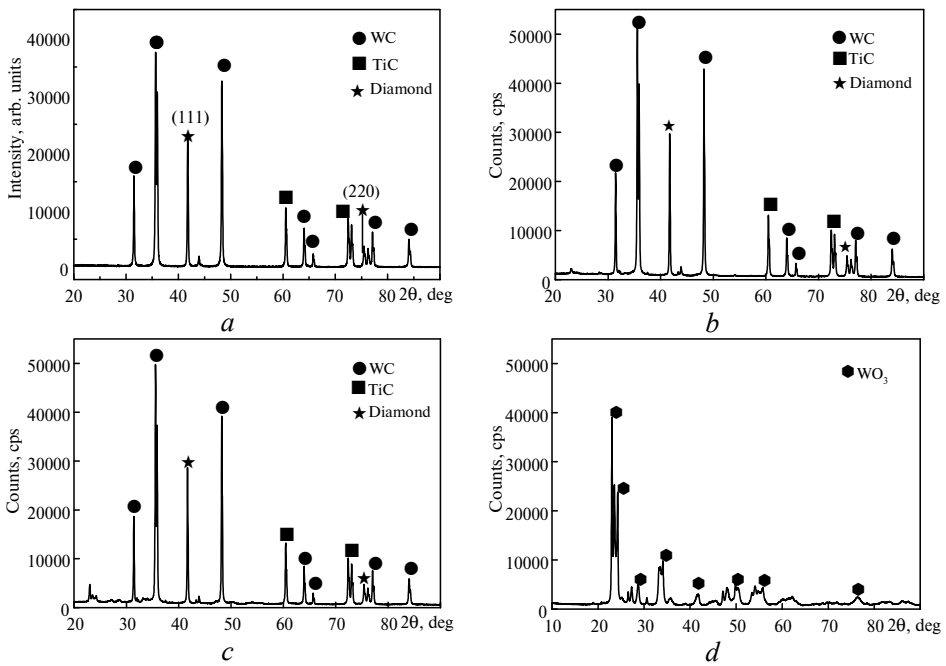

Fig. 2. XRD patterns of diamond films at normal temperature (*a*), 500 (*b*), 600 (*c*), 700 (*d*) °C.

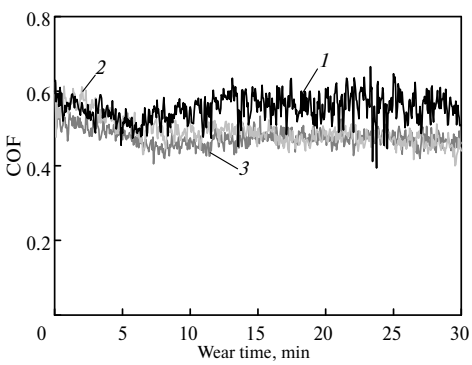

Fig. 3. COFs of diamond films vs wear time at different temperatures: 500 (*1*), 600 (*2*), 700 (*3*) °C.

Plane scans of worn track

Figure 4, *a* shows the plane scanned position of worn track at 500 °C. The film surface wore slightly, classified as slight adhesion wear. The plane scan result of

worn track is shown in Fig. 4, *b*. The mass fractions (wt %): C – 68.82, O – 13.93, Ti – 3.12, and W – 13.12; and the corresponding atom fractions (at %): C – 84.78, O – 12.88, Ti – 1.22, and W – 1.12. Figure 4, *c* shows that the C content was low on the worn track, and the wear was processed in the diamond film. Moreover, the O was detected on the worn tracks, and the O-rich regions appeared, as shown in Fig. 4, *f*. The W and Ti came from the chemical elements of substrate, as shown in Figs. 4, *d* and *e*.

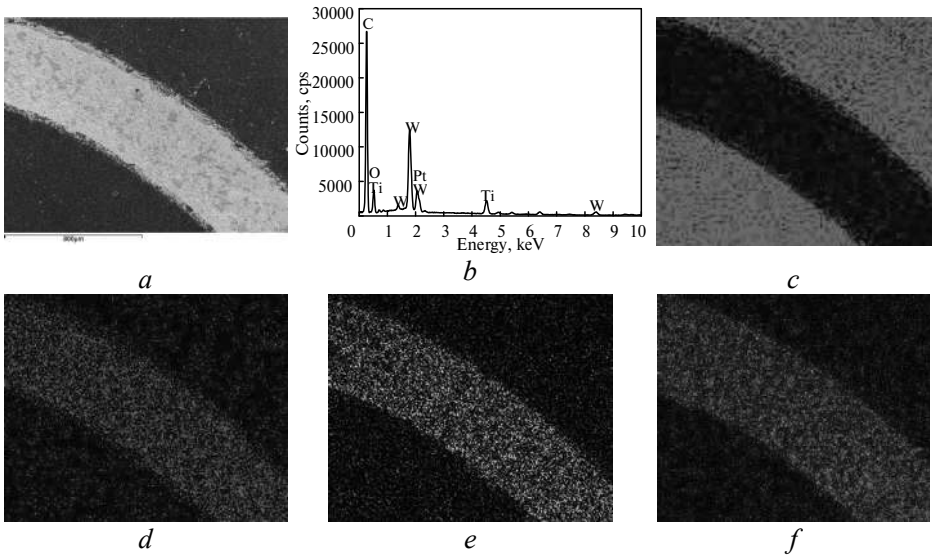

Fig. 4. Plane scans of worn track on diamond films after wearing at 500 °C: plane scanned position (*a*), result of plane scans (*b*), C (*c*), W (*d*), Ti (*e*), O (*f*) content.

Figure 5, *a* shows the plane scanned position of worn track at 600 °C. The wear was more serious than that at 500 °C. The plane scan result of worn track is shown in Fig. 5, *b*. The mass fraction (wt %): C – 69.71, O – 13.80, Ti – 2.47, and W – 14.39; and the corresponding atom fractions (at %): C – 85.04, O – 12.82, Ti – 0.94, and W – 1.20. The plane scan result of worn track at 600 °C was similar with that at 500 °C. It can be seen from Fig. 5, *c* that there was a little C element in worn track, and it gathered at non-wearing area that meant the diamond film was not oxidized seriously, the film was still intact and the chemical vapor deposited diamond film exhibited good oxidation resistance and wear resistance. In Figs. 5, *d* and *e* the colors of W and Ti at worn track were darker than them at non-wearing areas. Because the diamond film at worn track became thinner and X-ray of EDS could measure the substrate materials easily. Therefore, W and Ti enriched at worn track. The oxidation behavior at high temperature mainly occurred at worn track, so there was much O element at worn track, as shown in Fig. 5, *f*.

Figure 6, *a* shows the plane scanned position of worn track at 700 °C. Some furrows appeared at the center of worn track. The plane scan result of worn track is shown in Fig. 6, *b*. The mass fraction (wt %): C – 11.15, O – 22.99, Ti – 10.75, and W – 55.11; and the corresponding atom fraction (at %): C – 31.97, O – 49.44, Ti – 7.71, and W – 10.88. The C content on the worn track declined greatly compared with that at 600 °C, as shown in Fig. 6, *c*. This further explained the decreasing of C atom fraction on the worn track, the diamond film was completely oxidized, and the rest C existed in the form of TiC came from the substrate. The O content increased from 13.80 to 22.99 %, this was because the spalled debris that adhered on

the worn track was oxidized at 700 °C. Furthermore, the contents of W and Ti also increased significantly compared with that at 600 °C, as shown in Figs. 6, *d* and *e*, revealing that the substrate was exposed in the air and the diamond film was completely oxidized at 700 °C, the diamond film was failed due to oxidation.

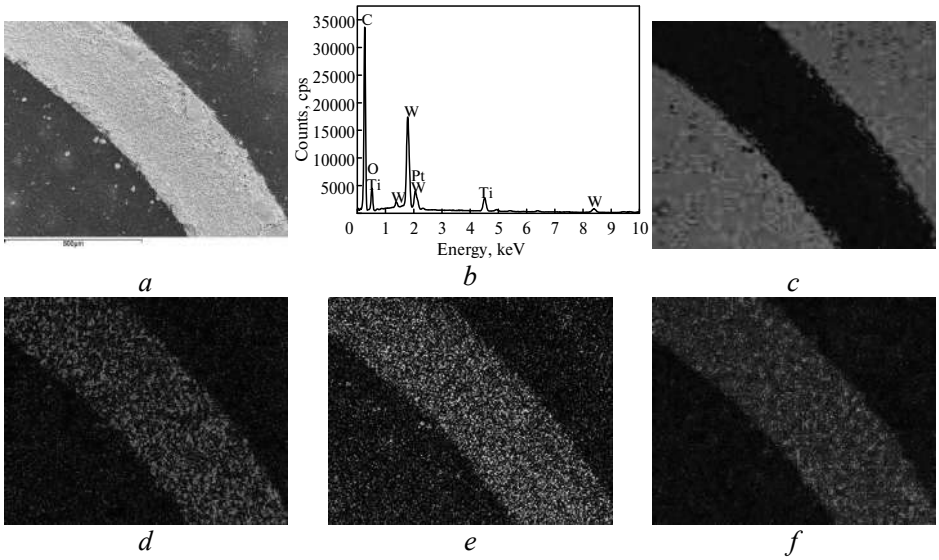

Fig. 5. Plane scans of worn track on diamond films after wearing at 600 °C: plane scanned position (*a*), result of plane scans (*b*), C (*c*), W (*d*), Ti (*e*), O (*f*) content.

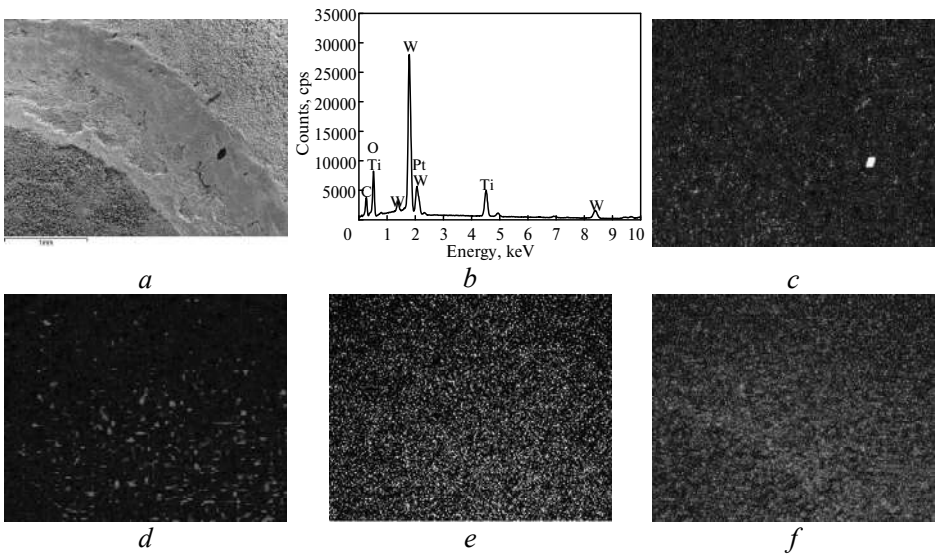

Fig. 6. Plane scans of worn track on diamond films after wearing at 700 °C: plane scanned position (*a*), result of plane scans (*b*), C (*c*), W (*d*), Ti (*e*), O (*f*) content.

Wear mechanism

Figure 7, *a* shows the worn morphology with the low magnification at 500 °C. As it was shown, some debris formed the small and numerous adhesion zones. The worn tracks were divided into debris adhesion and debris compaction. Figure 7, *b*

shows the worn morphology with the high magnification. The debris was produced and adhered on the worn surface in the wear test, which was not discharged and continuously compact under the cycle loads to form rough surface, revealing that the wear mechanism was primarily adhesion wear.

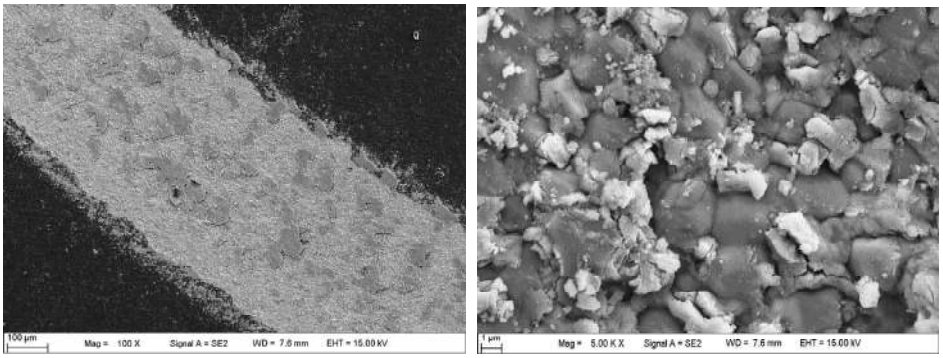

a *b*

Fig. 7. Morphologies of worn track on diamond film at 500 °C: low (*a*) and high (*b*) magnification.

Figure 8, *a* shows the worn morphology with the low magnification at 600 °C, it could be seen that some debris formed a large adhesion zone. Because the softer debris at 600 °C was helpful to form continual adhesion zone. Figure 8, *b* shows the worn morphology with the high magnification. The brittle fractures of diamond film were found on the worn track, showing that the fatigue stress led to cracking on the diamond film under the circular contact, and the cracks expanded gradually. Therefore, the diamond film produced the fracture phenomenon, showing a fatigue wear. The oxidation occurred preferentially on the grain boundaries at high temperatures, leaving a porous structure [22]. The SEM images further show that the rigid faces of diamond grains were retained after oxidation [23], some debris were dragged by the tribo–pair and stayed on the film surface.

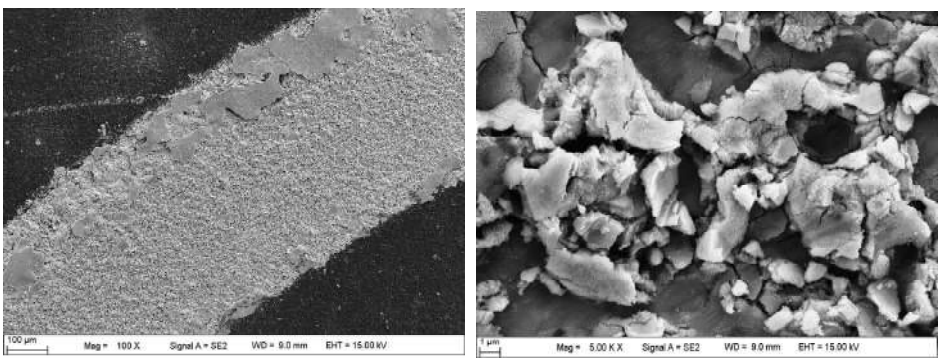

a *b*

Fig. 8. Morphologies of worn track on diamond film at 600 °C: low (*a*) and high (*b*) magnification.

Figure 9, *a* shows the worn morphology with the low magnification at 700 °C, and according to Fig. 6, *c*, the diamond film was completely oxidized. Figure 9, *b* shows the worn morphology with the high magnification. There were only massive WO_3 particles adhered on the diamond film surface, the diamond film was fully

oxidized and generated CO and CO_2. The WC on the substrate was reacted with the O_2 to produce the WO_3, which generated an amount of hard flaking debris during the brittle breaking under the load. During the oxidation, the O etched away the weak bonds of C on the grain boundaries and local defects. The C was evaporated from the defects and the non-diamond phase when the chemical vapor deposited diamond film was oxidized. Therefore, the WO_3 particles were formed on the substrate to accelerate the wear, the wear mechanism was abrasive wear. From the above analyses, the wear mechanism of diamond film at 700 °C was oxidation wear and abrasive wear, accompanied with adhesive wear and fatigue wear.

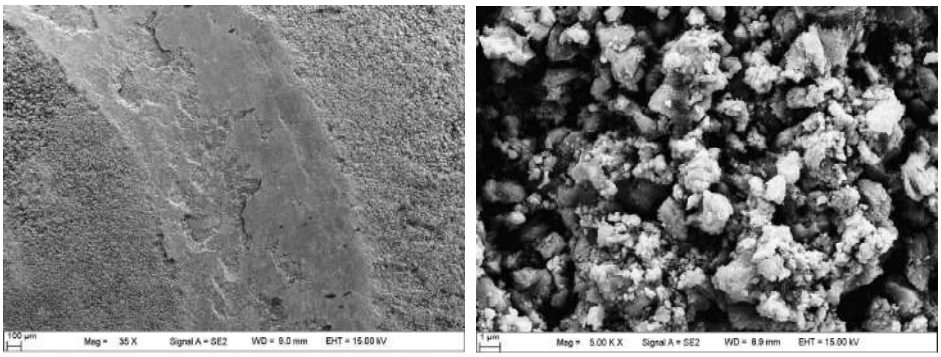

a *b*

Fig. 9. Morphologies of worn track on diamond film at 700 °C: low (*a*) and high (*b*) magnification.

CONCLUSIONS

At 500, 600 and 700 °C, the average COFs of diamond film are 0.55, 0.49 and 0.48, respectively, showing that the COFs decrease with the temperatures increasing.

The diamond film is oxidized completely at 700 °C, and generates CO and CO_2, which presents the film is failed.

The wear mechanism of diamond film at high temperature is primarily oxidation wear, adhesive wear and abrasive wear, accompanied with fatigue.

FUNDING

Financial support for this research by the Jiangsu Province Science and Technology Support Program (Industry) (BE2014818) is gratefully acknowledged.

Коефіцієнт тертя і характер зносу алмазних плівок, нанесених на ріжучий інструмент з твердого сплаву YT14 методом хімічного осадження з парової фази, досліджено високотемпературним трибометром при температурі 500, 600 і 700 °С. Результати показали, що вуглець алмазної плівки повністю вільний при 700 °С і утворює сполуки CO і CO_2. Площина (220) алмазної плівки окислюється при 500 °С, а площину (110) – при 700 °С. Середні коефіцієнти тертя алмазної плівки при 500, 600 і 700 °С становлять 0,55, 0,49 і 0,48 відповідно, механізмом зносу є переважно знос, викликаний окисленням, і абразивний знос, що супроводжується втомним і адгезійним зносом.

***Ключові слова**: хімічне осадження з парової фази, алмазна плівка, коефіцієнт тертя, висока температура, тертя і знос, механізм зносу.*

Коэффициент трения и характер износа алмазных пленок, нанесенных на режущий инструмент из твердого сплава YT14 методом химического осаждения из паровой фазы, были исследованы высокотемпературным трибометром при температуре

500, 600 и 700 °С. Результаты показали, что углерод алмазной пленки полностью свободен при 700 °С и образует соединения CO и CO_2. Плоскость (220) алмазной пленки окисляется при 500 °С, а плоскость (110) – при 700 °С. Средние коэффициенты трения алмазной пленки при 500, 600 и 700 °С составляют 0,55, 0,49 и 0,48 соответственно, механизмом износа является главным образом износ, вызванный окислением, и абразивный износ, сопровождаемый усталостным и адгезионным износом.

***Ключевые слова**: химическое осаждение из паровой фазы, алмазная пленка, коэффициент трения, высокая температура, трение и износ, механизм износа.*

1. Zhu R.H., Miao J.Y., Liu J.L., Chen L.X., Guo J.C., Hua C.Y., Ding T., Lian H.K., Li C.M. High temperature thermal conductivity of free-standing diamond films prepared by DC arc plasma jet CVD. *Diamond Relat. Mater*. 2014. Vol. 50. P. 55–59
2. Wei Q.P., Yu Z.M., Ashfold M.N.R., Ye J., Ma L. Synthesis of micro- or nano-crystalline diamond films on WC–Co substrates with various pretreatments by hot filament chemical vapor deposition. *Appl. Surf. Sci.* 2010. Vol. 256, no. 13, P. 4357–4364.
3. Vasconcellos de Siqueira Brandão L.E., Michels A.F., Camargo K.C., Balzaretti N.M., Horowitz F. Wet ability of PTFE coated diamond films. *Surf. Coat. Technol.* 2013. Vol. 232. P. 384–388.
4. Nasiekaa I., Strelchuk V., Boyko M., Voevodin V., Vierovkin A., Rybka A., Kutniy V., Dudnik S., Gritsina V., Opalev O., Strel'nitskij V. Raman and photoluminescence characterization of diamond films forradiation detectors. *Sens. Actuators A*: *Phys.* 2015. Vol. 223. P. 18–23.
5. Morales J., Apátiga L.M., Castaño V.M. Synthesis of diamond films from organic compounds by pulsed liquid injection CVD. *Surf Coat Technol.* 2008. Vol. 203, no. 5. P. 610–613.
6. Long H.Y., Luo H., Luo J.Q., Xie Y.N., Deng Z.J., Zhang X.W., Wang Y.J., Wei Q.P., Yu, Z.M. The concentration gradient of boron along the growth direction in boron doped chemical vapor deposited diamond. *Mater. Lett.* 2015. Vol. 157. P. 34–37.
7. Long H.Y., Li S., Luo H., Wang Y.J., Weia Q.P., Yu Z.M. The effect of periodic magnetic field on the fabrication and field emission properties of nanocrystalline diamond films. *Appl. Surf. Sci.* 2015. Vol. 353. P. 548–552.
8. Liu M.N., Bian Y.B., Zheng S.J., Zhu T., Chen Y.G., Chen Y.L., Wang J.S. Growth and mechanical properties of diamond films on cemented carbide with buffer layers. *Thin Solid Films*. 2015. Vol. 584. P. 165–169.
9. Iyuke S.E., Daramola M.O., Mokena P., Marshall A., Thermodynamic stability of graphitic diamond films produced from catalytic chemical vapor deposition reactor. *J. Ind. Eng. Chem.* 2015. Vol. 30. P. 336–341.
10. Cui Y., Zhang J.G., Sun F.H., Zhang Z.M. Si-doped diamond films prepared by chemical vapor deposition. *Trans. Nonfer. Met. Soc. China*, 2013. vol. 23, no. 10. P. 2962–2970.
11. Catena A., McJunkin T., Agnello S., Gelardi F.M., Wehner S., Fischer C.B. Surface morphology and grain analysis of successively industrially grown amorphous hydrogenated carbon films (a-C: H) on silicon. *Appl*. *Surf. Sci.* 2015. Vol. 347. P. 657–667.
12. Benarioua Y., Lesage J., Chicot D., Moisan M. Structure and hardness of diamond films deposited on WC–Co by CVD technique. *Surf. Coat. Technol.* 2013. Vol. 227, no. 29. P. 70–74.
13. Pu J.C., Wang S.F., Sung J.C. High-temperature oxidation behaviors of CVD diamond films. *Appl. Surf. Sci.* 2009. vol. 256, no. 3. P. 668–673.
14. Maida O., Tada S., Nishio H., Ito T. Substrate temperature optimization for heavily-phosphorus-doped diamond films grown on vicinal (001) surfaces using high-power-density microwave-plasma chemical-vapor-deposition. *J. Cryst Growth*. 2015. Vol. 424. P. 33–37.
15. Huang K., Hu X.J., Xu H., Shen Y.G., Khomich A. The oxidization behavior and mechanical properties of ultrananocrystalline diamond films at high temperature annealing. *Appl. Surf. Sci.* 2014. Vol. 317. P. 11–18.
16. Qian J., McMurray C.E., Mukhopadhyay D.K., Wiggins J.K., Vail M.A., Bertagnolli K.E. Polycrystalline diamond cutters sintered with magnesium carbonate in cubic anvil press. *Int. J. Refract. Met. Hard Mater*. 2012. Vol. 31, no. 3. P. 71–75.
17. Konicek A.R., Grierson D.S., Gilbert P.U.P.A, Sawyer W.G., Sumant A.V., Carpick R.W. Origin of ultralow friction and wear in ultrananocrystalline diamond. *Phys. Rev. Lett.* 2008. Vol. 23, no. 100. P. 1151–1156.
18. Sun X.F., Qiao Y.L., Song W., Ma S.N., Hu C.H. High temperature tribological properties of modified nanodiamond additive in lubricating oil. *Phys. Procedia*, 2013. Vol. 50. P. 343–347.

19. Shabani M., Abreu C.S., Gomes J.R., Silva R.F., Oliveira F.J. Effect of relative humidity and temperature on the tribology of multilayer micro/nanocrystalline CVD diamond coatings. *Diamond Relat Mater*. 2017. Vol. 73. P. 190–198.
20. Liu S., Liu J.L., Li C.M., Guo J.C., Chen L.X., Wei J.J., Hei L.F., Lu F.X. The mechanical enhancement of chemical vapor deposited diamond film by plasma low–pressure/high–temperature treatment. *Carbon*. 2013. Vol. 65, no. 12. P. 365–370.
21. Ueda K., Kasu M., Tallaire A., Makimoto T. High-pressure and high-temperature annealing effects on CVD homoepitaxial diamond films. *Diamond Relat. Mater.* 2006. Vol. 15, no. 11–12. P. 1789–1791.
22. Liu J.M., Lv. X. Oxidation behavior of high quality freestanding diamond films. *Trans. Mater. Heat Treat.* 2007. Vol. 28, no. 2. P. 89–93.
23. Chen N.C., Ai J., Chen Y.C., He P., Ren J.X., Ji D.M. Multilayer strategy and mechanical grinding for smoothing CVD diamond coated defective substrate. *Mater. Design*. 2016. Vol. 103. P. 194–200.

Received 23.01.18
Revised 04.04.18
Accepted 04.04.18